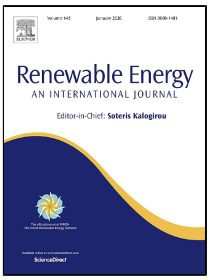

Experimental and numerical analysis of a backpressure Banki inline turbine for pressure regulation and energy production

Marco Sinagra, Costanza Aricò, Tullio Tucciarelli, Gabriele Morreale

PII:	S0960-1481(19)31567-8
DOI:	https://doi.org/10.1016/j.renene.2019.10.076
Reference:	RENE 12445
To appear in:	*Renewable Energy*
Received Date:	01 March 2019
Accepted Date:	15 October 2019

Please cite this article as: Marco Sinagra, Costanza Aricò, Tullio Tucciarelli, Gabriele Morreale, Experimental and numerical analysis of a backpressure Banki inline turbine for pressure regulation and energy production, *Renewable Energy* (2019), https://doi.org/10.1016/j.renene.2019.10.076

Experimental and numerical analysis of a backpressure Banki inline turbine for pressure regulation and energy production

Marco Sinagra[a,*], Costanza Aricò[a] ,Tullio Tucciarelli[a], Gabriele Morreale[b]

[a] Dipartimento di Ingegneria, Università degli Studi di Palermo, Italy
[b] WECONS company, Palermo, Italy

*Corresponding author
E-mail addresses: marco.sinagra@unipa.it (M. Sinagra), costanza.arico@unipa.it (C. Aricò), tullio.tuciarelli@unipa.it (T. Tucciarelli), g.morreale@wecons.it (G. Morreale)

Abstract

Water distribution networks have become, in recent years, a major opportunity for the harvesting of renewable energy, which is otherwise dissipated though hydrovalves installed for discharge and pressure regulation. Mini and micro hydroturbines have the capability of providing the same functionality of hydrovalves, producing at the same time a relevant amount of electric power. In this paper a 10 kW prototype of a new compact in-line turbine, named Power Recovery System (PRS), has been designed, constructed and tested in the hydraulic laboratory of the University of Palermo. The proposed device is a Banki-type micro-turbine, with positive outflow pressure and a mobile regulating flap for hydraulic control of the characteristic curve. The device is aimed to control pressure or discharge inside a water transport or distribution network, while producing energy with good efficiency values, up to 76%. Using two pressure meters located immediately before and after the turbine, it is possible to control the net head with given discharge (passive mode) or to control discharge by regulating the net head (active mode). 3D numerical analysis and laboratory measurements provide a low variation of efficiency for different positions of the mobile flap, especially for low variations in discharge.

Keyword: Pressure control , Micro-hydropower, Energy recovery, Water distribution network, Banki turbine, Energy harvesting

1. Introduction

Micro-turbine, Pressure Reducing Valves (PRV) and needle valves, installed in Distribution or Transport Water Networks, have different functions. PRVs are aimed to control pressure in the conduit for a given demand and needle valves are aimed to control discharge given fixed outlet pressure [1]-[5]. Micro-turbines are aimed to produce electric energy and are often installed in the conduit immediately before open water tanks to allow free outlet discharge [[6]-[12]. The founding mechanism is the same

for all devices; PRVs and needle valves dissipate energy to control pressure or discharge, while micro-turbines transform the mechanical energy of the water in electricity. Installation of PRVs and needle valves of course hampers installation of micro-turbines and, with that, the opportunity to take advantage of the lost hydraulic energy.

A large literature is available on the use of Pumps As Turbines (PATs) for the achievement of all the previous tasks [13]-[16], even for small discharges as in the case of high-rise buildings [17]. The major merit of PATS is the low commercial cost of the device [18], even if this cost is often only a small fraction of the direct and indirect costs required for actual electricity production [19]. A first drawback of PATS is the relatively large volume required to host the turbine, the generator, the piping and all the control system. A second drawback is limited average efficiency, occurring especially in the case of high variable discharge and pressure, mainly due to the lack of mobile parts for control of the characteristic curve. In addition, PATs suffer from tip leakage vortex (TLV) [[20]-**Error! Reference source not found.**, and the occuring vortices affect the production efficiency and the operation stability [[20]-**Error! Reference source not found.**.

Other types of traditional turbines, like the Francis one, usually have high installation and maintenance costs [25],[26] that largely outweigh the possible benefit. Recently, small hydro-turbines with tubular propeller [27], also with counter-rotating runners [[28],[29]], have been proposed. The advantage of the proposed device is that its impeller can be located inside the pipe. In both devices mobile parts for an efficient control of the characteristic curve are missing, like in the PATs.

Banki or Cross-Flow turbines are a good alternative to PATs and to other types of micro-turbines [[8],[12]]. They are small in size and their axis is orthogonal to the pipe direction. This implies that the flow direction always remain in the vertical plane including the pipe axis. Moreover, a simple mobile flap can control the size of the inlet impeller surface, to change the characteristic curve with a small efficiency reduction, especially in the case of constant discharge and variable net head.

Banki turbines were originally designed for free outlet conditions, to be installed in the final section of an aqueduct serving an open water tank. Traditional Banki turbines had low efficiency, but new advances in their design criterion have allowed achievement of very high values, claimed to be up to 90% [29]. Recently, a new type of Banki turbine named PRS for positive outflow pressure has been proposed [[30],[31]]. The new device has the simplicity of Banki turbines for free outflow, but can be installed inline and has good hydraulic efficiency, almost always over 70%. The proposed device can be set in the ‘passive’ or ‘active’ mode. When the device is set in the ‘passive’ mode this allows:

1) setting the outlet piezometric level at any required value, lower than the inlet one, but even much greater than the ground elevation, while also being variable in time;
2) transforming the inlet-outlet hydraulic power difference into electricity;
3) measuring the flow rate.

When the device is set in the 'active' mode it provides discharge regulation by fixing the outlet piezometric level corresponding to the required discharge in the accomplishment of function 1), also replacing function 3) with pressure metering.

In previous works a PRS turbine prototype, lacking the regulating flap, was tested in the lab [[30]], while the functionality of the same flap was numerically validated using 2D CFD simulations [[31]]. In the context of the 'Pressure Management System - PMS' project, funded by the Italian government, a set of different PRS turbine prototypes was designed, constructed and tested in the laboratory of the University of Palermo. In the following sections, experimental and numerical results relative to the first prototype are compared to highlight the potentialities and the technical challenges of the proposed device.

2. Turbine design

The new turbine generates hydropower through a Banki type impeller, with a mobile regulation flap and a pressurized diffusor. The blades have cylindrical geometry, and a guide line with constant curvature. The blades link two disks and one of these disks provides the torque for the shaft generator. Flow enters the channels between the blades through the inlet surface given by a first part of the cylinder defined by the external circle of the two disks as a guideline and leaves the impeller through a second part of the same cylindrical surface. Both the inlet and the outlet surfaces underpin an angle λ_{max} that can range between 90 and 120 degrees, according to the particular machine. The regulation flap can partially close the inlet surface when a reduction of the discharge occurs without a corresponding head reduction, in order to keep the optimal velocity ratio constant between the inlet particle velocity and the impeller rotational velocity at the same inlet surface. Fig.1 shows a sketch of the turbine. The diffusor guarantees gradual variation of the particle velocity direction and is connected to the outlet pipe, which has the same axis as the inlet one. Preliminary laboratory tests on the turbine with pressurized diffusor, without the application of the regulation system, are described in [30].

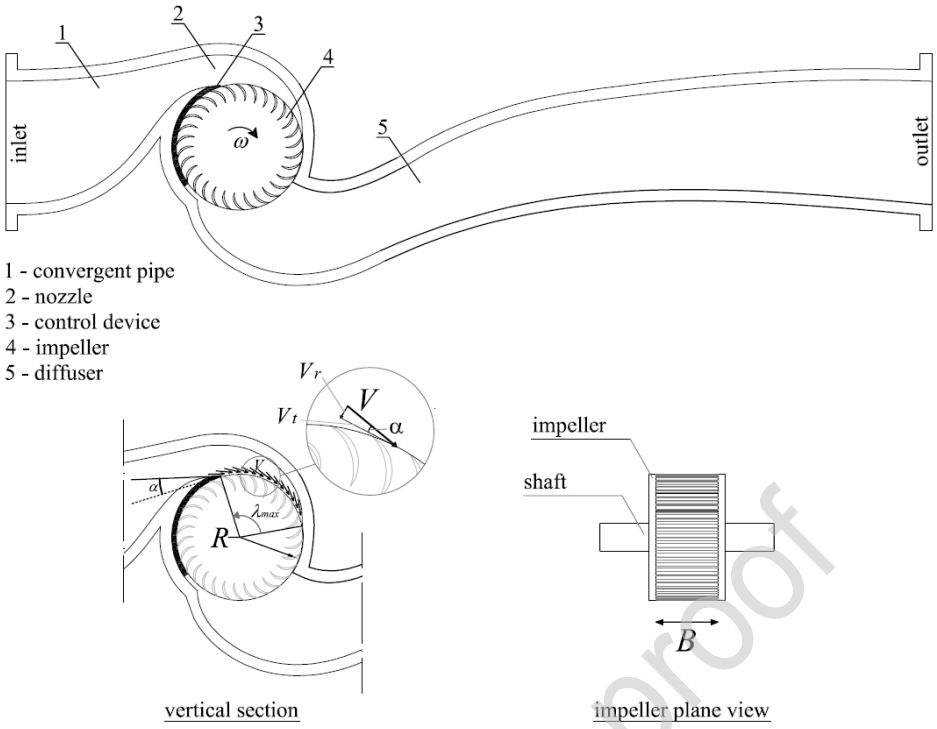

Fig. 1. Vertical section of a pressurized Cross-Flow turbine.

In previous studies [8] Sammartano et al. showed that Banki turbine efficiency is mainly a function of two parameters: 1) the velocity ratio V_r, given by the ratio between the tangent component of the inlet velocity and the reference system velocity at the impeller inlet surface; 2) the λ angle. The efficiency always drops along with λ and, in Banki turbines with free outflow, attains the maximum value for $V_r \approx 2$ and $\lambda=\lambda_{max}$, where

$$V_r = \frac{V \cos\alpha}{\omega R} \tag{1}.$$

Experimental evidence [31] has shown that the maximum efficiency, in pressurized Banki turbines, is obtained with a smaller velocity ratio, a function of the λ angle, but approximately equal to 1.7.

Turbine design is based on the relationship among the rotational velocity ω, the inlet velocity V and the net head ΔH occurring at the maximum efficiency condition. Previous studies [25],[31] have shown that this relationship, according to the results of extended 2D simulations, is given by:

$$V = C_V \sqrt{2g\left(\Delta H - \xi \frac{\omega^2 D^2}{8g}\right)} \tag{2},$$

where C_v= 0.98, ξ=1 in the case of free outlet flow or ξ=2.1 in the case of pressurized outflow.

The turbine impeller can be designed to be used in both the active and passive modes, after setting 1) the design discharge Q_d sought after at the fully open regulating condition ($\lambda=\lambda_{max}$) and 2) the design net head ΔH_{max} available in the turbine location for the discharge Q_d. One of two options must be preliminarily chosen. Option 1 is to fix the *B/D* ratio, where *B* is the impeller width (see Fig.1), and to compute the corresponding optimal rotational velocity ω; option 2 is to fix the rotational velocity ω and to compute the *B* and *D* parameters in order to get the optimal relative velocity 1.7 at the angle $\lambda=\lambda_{max}$. The second option is usually preferred because it allows preliminary selection of the electric generator.

In both cases momentum equation (2) is coupled with the relative velocity optimality condition, which provides:

$$\frac{0.85\omega D}{\cos\alpha} = V \tag{3},$$

where α is the velocity inlet angle with respect to the tangent direction. The mass continuity requirement provides the second constraint:

$$Q = \frac{BD\lambda_{rmax} V \sin\alpha}{2} \tag{4}.$$

Equations (2), (3) and (4) can be solved in the *V*, *D*, ω unknowns according to hypothesis (1) and to *V*, *D*, *B* unknowns according to hypothesis (2). A more extended discussion about the turbine design and management criteria can be found in [16].

The previous design procedure provides the fundamental parameters of the turbine geometry, but there is a big gap between the executive design and the previous results. Other major geometrical parameters, like the ratio between the internal and the external disk diameters, or the number of blades, were previously investigated by the same authors using both laboratory experiments and CFD simulations for the case of traditional free-outflow Banki turbines, and using only CFD simulations for backpressure Banki turbines. Moreover, almost all the theoretical studies available in the literature do not take into account the effect of blade and flap thickness on the turbine efficiency. Because mechanical failure of Banki type turbines is one of the major complaints coming from users, it is quite important to carry out CFD and laboratory experiments in the search for a motivated choice of all the geometric parameters of the proposed device.

3. Experimental facility and Prototype

Experiments were performed in the hydraulic laboratory of the Engineering Department of the University of Palermo (Italy). The experimental facility is made up of a water pumping system and a test stand with the turbine prototype coupled with a synchronous generator connected to a resistive load. The pumping system provides the inlet pressure and the flow rate for the prototype turbine. The system operates in closed-loop mode and is formed by a water pressure booster pump unit, an open tank reservoir, a suction pipe, a supply pipe, a bypass pipe, a return pipe and three manual valves which allow one to regulate both the flow rate and the pressure at the turbine inlet. In Fig. 2 a section of the experimental facility is shown.

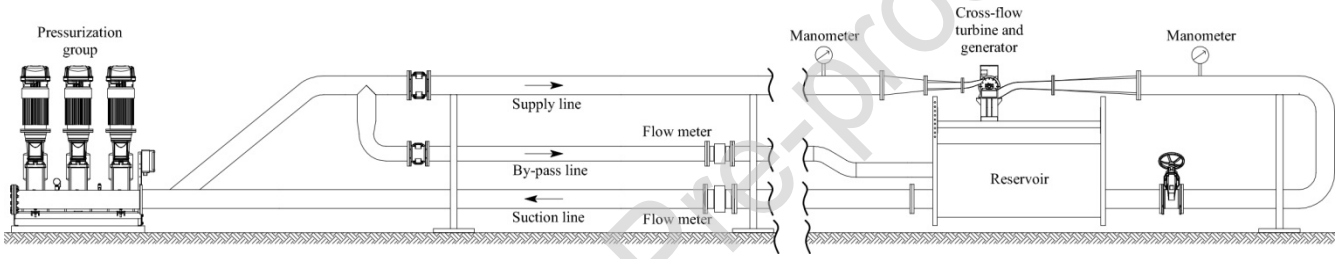

Fig. 2. The experimental facility.

The pressure booster unit has a pressure regulation range from 1 to 6 bar, and an operation range from 5 l/s to 50 l/s. The flow rate in the pumping system is measured by three flow meters installed in the suction, supply and by-pass pipes. The turbine prototype is coupled with a generator, a torque-meter and two digital manometers. The test bench monitoring instrumentation and the corresponding measurement error can be found in [30].

The turbine prototype designed using the described procedure is made of cast iron. The impeller, made of stainless steel, has 45 semicircular blades [32] connected each other by a couple of circular plates fixed to the shaft, which rotates on two bearings; the impeller has no internal shaft. The flap is made of stainless steel and it is moved by a linear electrical actuator. Parameters D and B were calculated by setting the angular velocity equal to 1500 rpm. According to the procedure described in paragraph 2, the D impeller diameter was 133 mm and the B impeller width was 59 mm. The total length of the turbine, measured between the input and output flanges, is 90 cm. In Fig. 3 the turbine prototype installed in the experimental facility is shown.

Fig. 3. Test stand with the turbine prototype.

The hydraulic performance of the turbine depends on the shape of the impeller blades. Specifically, when the blades thickness is reduced, the hydraulic performance increases. However, the blades must resist water thrust and fatigue, which is subjected to a cyclic load. In the turbine prototype the front surface of the blade was designed according to the procedure described in [33]. With regard to the back surface, a finite element method (FEM) was applied by assigning the maximum pressures, obtained with a preliminary CFD analysis, on the most stressed blade, to estimate the maximum stress. Assuming the stress-cycle pattern shown in Figure 4 for an austenitic steel, the blade thickness was chosen so as to obtain a maximum stress from the FEM analysis lower than 100 MPa. This condition makes it possible to retain the blade resistant up to an infinite number of cycles.

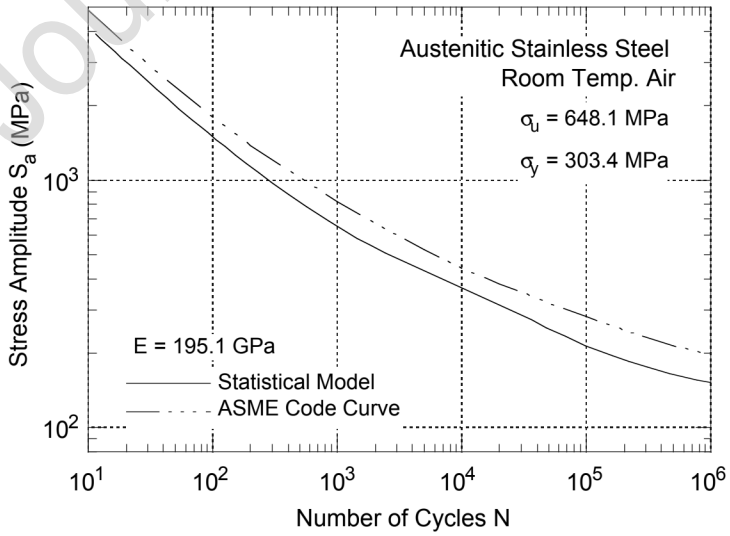

Fig. 4. Fatigue design curves [34].

The FEM analysis carried out on the rotor prototype showed that, for a thickness blade equal to 2 mm, the stress concentration occurs at the root of the blade, where it is most possible that fatigue damage may occur, and that the maximum stress value is 63 MPa (Fig. 5), which is compatible with an infinite number of cycles.

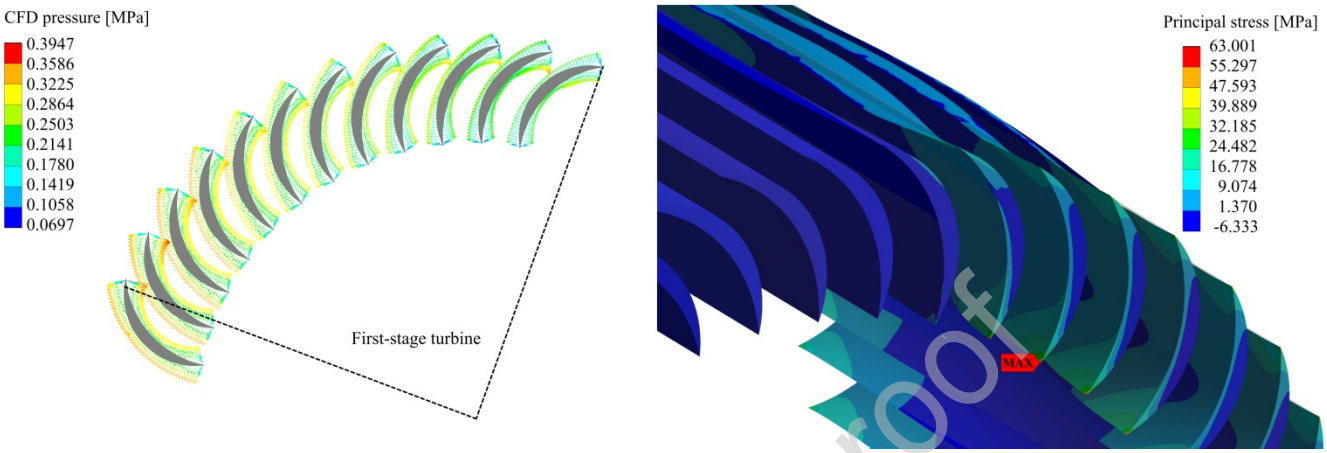

Fig. 5. CFD results as loads in FEM analysis (left); Blades stress contour (right).

4. CFD simulations

Experimental results were compared with 3D numerical simulations carried out by means of the commercial solver ANSYS® CFX. The computational domain was divided into two physical sub-domains: the rotor (impeller) and the stator, made up of the nozzle and the casing of the turbine. Each sub-domain was discretized by into tetrahedral and prismatic elements: 12,351,750 in the rotor domain and 4,906,676 in the stator domain (Fig. 6).

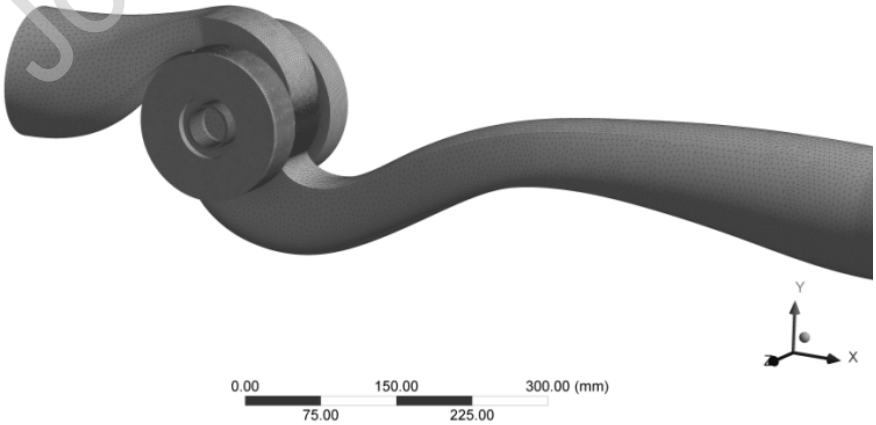

Fig. 6. Prototype fluid domain discretization.

The selected turbulence model was the RNG k-epsilon model, based on Re-Normalization of the Navier-Stokes equations. Simulations were performed in unsteady state condition and the interface model between stationary and rotating domain is transient rotor-stator type. The time step used for each run is 2.5×10^{-4} s. The root mean square residual was used for the convergence criterion with a residual target equal to 1.0×10^{-5}.

The boundary conditions selected in the simulations according to the experimental data are the following: a) the total pressure per unit weight at the nozzle inlet, corresponding to the piezometric level plus the kinetic energy per unit weight, b) the flow rate at the outlet section of the casing. The initial condition for each unsteady state simulation is the fluid field output computed according to the steady state flow assumption. Due to the large computational effort required for each simulation (about 15 days) only three points were found, corresponding to different positions of the flap and discharges. In Figs. 8 and 9 the efficiency of the turbine and the net head, estimated in each numerical simulation, are shown along with the experimental results. The capability of the numerical model to well predict these two parameters is fundamental for validation of the designed turbine in real field applications.

5. Laboratory and CFD results

The experimental tests were carried out by measuring the efficiency and the net head of the turbine prototype for each flap position and given discharge. The flow rate changed in the range 5.9-30 l/s and the flap position changed in the range 30°- 90° of the impeller inlet angle. The rotational velocity ω was selected by regulating the electric load connected to the generator in order to maximize the efficiency corresponding to the given flow rate. The test results are shown in table 1.

Table 1
Experimental results.

λ [°]	Q [l/s]	ΔH [m]	ω [rpm]	η [%]	λ [°]	Q [l/s]	ΔH [m]	ω [rpm]	η [%]
90	29.5	26.5	1175	73.6	50	23.0	29.2	910	60.0
90	28.7	23.2	1203	70.7	50	20.4	23.5	845	58.7
90	23.3	15.1	962	68.7	50	15.9	16.0	914	62.7
90	17.3	8.3	721	64.7	50	9.9	6.3	546	52.0
90	10.8	2.4	432	55.6	40	17.0	26.1	772	54.6
65	26.0	23.3	1056	69.0	40	14.8	21.7	1059	54.8
65	22.1	17.2	926	68.0	40	12.0	15.2	885	53.0
65	17.2	10.8	714	65.5	40	9.8	9.7	735	51.6
65	10.0	3.4	394	51.5	40	6.9	4.7	429	33.0
60	24.9	25.2	1034	67.5	30	11.5	24.1	882	46.7
60	21.9	19.6	909	66.3	30	9.2	15.1	868	46.0
60	14.5	9.2	638	63.6	30	8.1	13.2	946	42.0
60	10.2	4.3	424	53.2	30	5.3	5.0	415	30.0

In Fig. 7 the experimental characteristic curves of the turbine are shown. The graph shows that the turbine attains a maximum efficiency equal to 76%, for a discharge equal to 30 l/s, with the flap in fully open conditions. The graph also shows that, in the passive mode, the flap mobility makes it possible to save a constant net head for hydroelectric production within a large range of possible discharges. Similarly, in the active mode the flap position makes it possible to convey the sought-after discharge by changing the head jump provided by the turbine. These characteristics of the turbine are essential for installations inside water supply networks, because in many instances they can provide the same functionality as PRVs. Comparison of the numerical results (black points in the graph) and the experimental data shows that the CFD 3D model is well able to predict the net head as a function of discharge and position (Fig. 7), with an error of 1.5%.

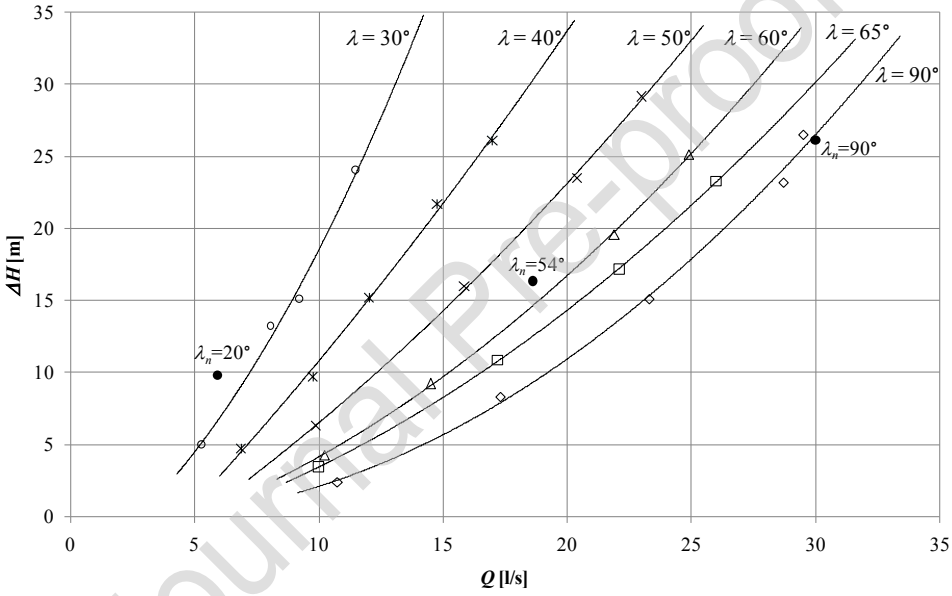

Fig. 7. Prototype characteristic curve for each flap position.

We can observe that the experimental iso-efficiency curves (Fig. 8) show a steeper reduction of the efficiency along with the discharge Q than the net head ΔH. Sammartano et al. have shown in [35] that the efficiency reduction can be mainly related to the reduction of the λ angle and to the difference of the velocity ratio with respect to the optimal one. In this case the velocity ratio is kept almost constant by the rotational velocity regulation and the efficiency reduction can be attributed almost entirely to the λ reduction. Momentum Eq. (2) shows that the velocity change is proportional to the root of ΔH minus the square of the optimal rotational velocity, which increases along with ΔH. This implies that, in the case of constant discharge, the velocity increment is much lower than the net head increment, along with the corresponding inlet λ angle reduction. In the case of a constant net head, the λ reduction is

instead simply proportional to the required discharge reduction and this explains the different efficiency slopes along the ΔH and Q directions.

The reduction of efficiency along with the λ angle is mainly due to the smaller torque provided by the blades at the proximity of the inlet and outlet impeller surface. Smaller λ angles reduce the ratio between the partially and the fully operating channels and this reduction is further enhanced by the thickness of the blades. More constant efficiencies could be obtained by increasing the number of blades and reducing their thickness, but this would imply much higher manufacturing costs. Finally observe that the flap is a constructively simple device and does not require complex kinematic movements, but only a linear actuator. The cost of the flap system is lower than one tenth of the total cost of the prototype.

The best efficiency point (BEP) was achieved for hydraulic conditions almost coincident with the design point parameters: the maximum efficiency η_{max} was 76.3% for a water discharge Q = 29.5 l/s, a net head ΔH of 26.5 m, the impeller inlet angle λ=90° and a velocity ratio V_{ratio} = 1.7. The maximum efficiency was obtained with a ratio V_{ratio} equal to the design value. The minimum turbine efficiency was found to be equal to η_{min} = 30%, which occurred for the minimum water discharge, Q_{min} = 5.3 l/s. The minimum efficiency was obtained with a flow rate equal to 17% of the design discharge value.

Comparison of the numerical results (black points in the graphs of Figg. 7 and 8) and the experimental data shows that the CFD 3D model is well able to predict the relationship among the discharge, the net head and the hydraulic efficiency occurring inside the turbine. The small overestimation of the numerical efficiency with respect to the experimental data is due to the friction of seals and bearings, not accounted for in the CFD analysis. Observe that the energy dissipation due to the friction of mechanical components is mainly a function of the rotational velocity of the impeller and is almost independent of the gross power produced. This explains the larger difference existing in Fig 8 between the efficiencies measured and computed at points ΔH,Q corresponding to smaller powers.

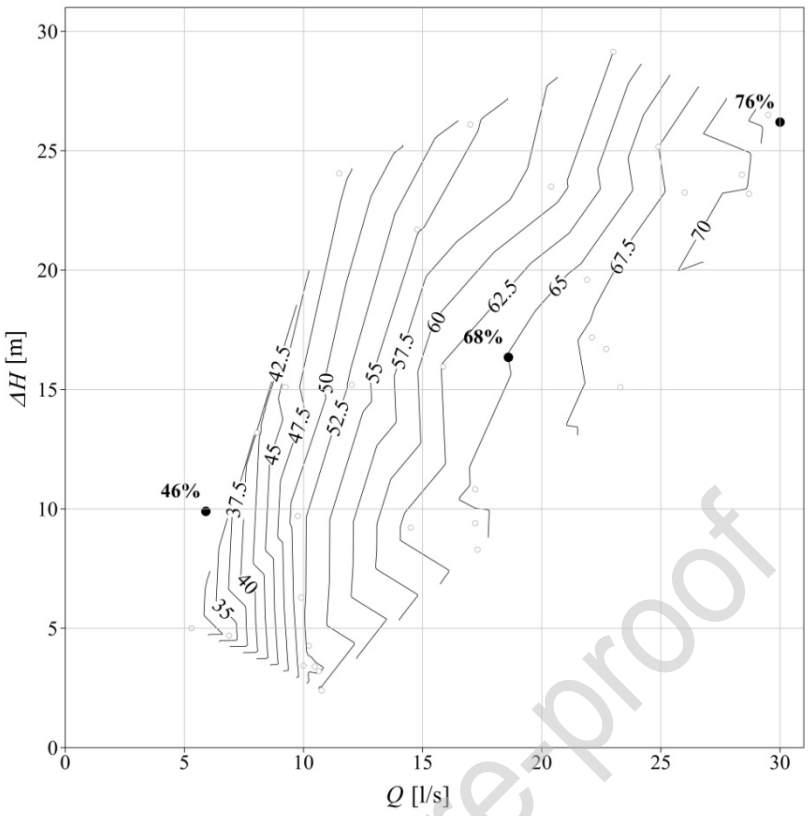

Fig. 8. Efficiency contour.

The experimental results showed that the PRS is able to easily adapt its characteristic curve to the changes of the flow rate Q and the net head ΔH occurring in a water network. This peculiarity differentiates the PRS from the PAT. Although the PAT can be coupled to electronic systems for regulation of the rotational velocity, the resulting change of the characteristic curve would easily lead to efficiencies that are much smaller than the efficiencies achieved around the design point. To avoid this drawback, a hydraulic regulation system is coupled to the electric one and the latter is only used to save the maximum efficiency. This requires either dissipating energy out of the turbine or bypassing part of the flow rate [36].

A simple quantitative comparison can be made between the performance of the PRS tested in the lab and a PAT with a similar characteristic curve [37], when they are put at the end of a hypothetical pipeline where fully turbulent flow occurs, feeding a distribution network from an open water tank 30 m higher (Fig. 9).

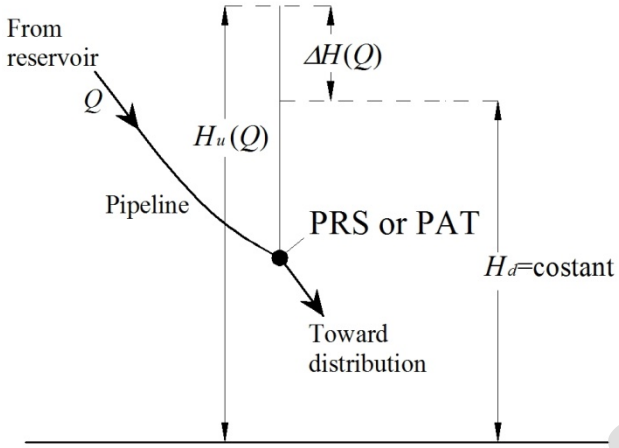

Fig. 9. Hypothetical installation scheme.

Assume the PAT design working point to be Q=22 l/s, ΔH= 8.3 m, with a produced output power equal to 1.20 kW. In the same condition the PRS would produce a similar power. Assume that, due to a demand reduction, the flow rate drops up to 11 l/s; in this case the net head at the end of the pipeline would rise up to 24.0 meters due to the smaller head losses along the pipeline. Because this point is out of the PAT characteristic curve, using the PAT we need to dissipate part of the hydraulic energy upstream of the turbine and the output power, according to the characteristic curves shown in [37] and not reported here for brevity, would only be 0.20 kW. On the other hand, the output power of the PRS would be about six times higher than that of the PAT, equal to 1.18 kW. This implies that, in the case of a large variation of the flow rate during hydropower production, the total amount of produced energy is likely to be much greater for the PRS than for the PAT.

6. Conclusions

The prototype of a Banki-type turbine with back-pressure in the outlet cross-section, called the PRS, was validated and tested. The PRS is equipped with an internal setting flap making it possible to change the characteristic curve of the turbine, saving good efficiency within a large discharge range. Hydraulic tests showed that the PRS could be used in water distribution networks for regulation of the flow rate, as an alternative to needle valves, or for regulation of the downstream head, as an alternative to PRV valves. The PRS, like other device with mechanical rotating parts, has construction and management costs that are of course larger than the costs of PRV or other valves. This implies that a cost/benefit analysis is always in order to evaluate the real convenience of its installation [38]. A large

industrial and research effort is still required to achieve smaller installation and management costs, without losing the possibility of large energy production.

The prototype tested in the lab was simulated using a 3D CFD analysis. Because each simulation took 15 days in a single multi-core PC, only a few points were computed. Comparison between experimental and numerical results is of paramount importance, because it confirms the quality of the prediction carried out by the model and allows its use for initial validation of further modifications of the proposed device.

Optimal efficiencies were obtained by varying the impeller rotation speed along with the net head, using a synchronous generator in the lab facility. In real water distribution networks, impeller rotation speed variation is only possible by coupling an inverter to the electric generator. This implies an additional cost, which has to be compared to the increment of energy production, as already proposed in [19].

Because of the long time occurring between the hydropower plant design and its actual installation, water managers often change their management rules before or during the actual energy production. This implies that the capability of changing the characteristic curve of the turbine, still keeping good efficiency values, can be quite important for investors. See, for instance, the installation and testing of a PRS in a real water transport network presented by Sinagra et al. [39].

References

[1] S. Nazif , M. Karamouz, M. Tabesh, A. Moridi, Pressure Management Model for Urban Water Distribution Networks. Water Resources Management 24 (2010) 437–458.
[2] L. Araujo, H.M. Ramos, S. Coelho, Pressure control for leakage minimization in water distribution systems management. Water Resources Management 20(1) (2006) 133–149.
[3] J. Almandoz, E. Cabrera, F. Arregui, E. Cabrera, R. Cobacho, Leakage Assessment through Water Distribution Network Simulation. Journal of Water Resources Planning and Management 131(6) (2005) 458–466.
[4] T. Tucciarelli, A. Criminisi, D. Termini, Leak Analysis in Pipeline Systems by Means of Optimal Valve Regulation. Journal of Hydraulic Engineering 125(3) (1999) 277–285.
[5] S. Prescott, B. Ulanicki, Improved Control of Pressure Reducing Valves in Water Distribution Networks. Journal of Hydraulic Engineering 134(1) (2008) 56–65.
[6] B. Coelho, A. Andrade-Campos, Energy Recovery in Water Networks: Numerical Decision Support Tool for Optimal Site and Selection of Micro Turbines, Journal of Water Resources Planning and Management 144 (3) (2018).
[7] S. Khosrowpanah, M. Albertson, A.A. Fiuzat, Historical overview of Cross-Flow turbine. Int Water Power Dam Constr. (1984) 38–43.
[8] V. Sammartano, C. Aricò, M. Sinagra, T. Tucciarelli, Cross-Flow Turbine Design for Energy Production and Discharge Regulation. Journal of Hydraulic Engineering 141(3) (2014).

[9] O. Fecarotta, C. Aricò, A. Carravetta, R. Martino, H.M. Ramos, Hydropower Potential in Water Distribution Networks: Pressure Control by PATs. Water Resources Management 29(3) (2014) 699-714.
[10] M. De Marchis, B. Milici, R. Volpe, A. Messineo, Energy Saving in Water Distribution Network through Pump as Turbine Generators: Economic and Environmental Analysis. Energies 9(11) (2016).
[11] A. Carravetta, G. Del Giudice, O. Fecarotta, H.M. Ramos, PAT Design Strategy for Energy Recovery in Water Distribution Networks by Electrical Regulation. Energies 6(1) (2013).
[12] M. Sinagra, V. Sammartano, C. Aricò, A. Collura, Experimental and Numerical Analysis of a Cross-Flow Turbine. Journal of Hydraulic Engineering 142(1) (2016).
[13] N. Fontana, M. Giugni, L. Glielmo, G. Marini, R. Zollo, Hydraulic and electric regulation of a prototype for real-time control of pressure and hydropower generation in a water distribution network, Journal of Water Resources Planning and Management, 144(11) (2018).
[14] A. Muhammetoglu, I.E. Karadirek, O. Ozen, H. Muhammetoglu, Full-scale PAT application for energy production and pressure reduction in a water distribution network, Journal of Water Resources Planning and Management, 143(8) (2017).
[15] A. Carravetta, O. Fecarotta, M. Sinagra, T. Tucciarelli, Cost-Benefit Analysis for Hydropower Production in Water Distribution Networks by a Pump as Turbine, Journal of Water Resources Planning and Management 140(6) (2014).
[16] O. Fecarotta, C. Aricò, A. Carravetta, R. Martino, H.M. Ramos, Hydropower Potential in Water Distribution Networks: Pressure Control by PATs. Water Resources Management 29(3) (2014) 699-714.
[17] J. Du, H. Yang, Z. Shen, J. Chen, Micro hydro power generation from water supply system in high rise buildings using pump as turbines, Energy 137 (2017) 431-440.
[18] D. Novara, A. Carravetta, A. McNabola, H.M. Ramos, Cost model for Pumps As Turbines in run-of-river and in-pipe micro-hydropower applications, Journal of Water Resources Planning & Management 145(5) (2019) 1-9.
[19] V. Sammartano, P. Filianoti, M. Sinagra, T. Tucciarelli, G. Scelba, G. Morreale, Coupled hydraulic and electronic regulation of cross-flow turbines in hydraulic plants, Journal of Hydraulic Engineering 143(1) (2017).
[20] Y. Liu, L Tan, Spatial–Temporal Evolution of Tip Leakage Vortex in a Mixed-Flow Pump With Tip Clearance, Journal of Fluids Engineering 141(8) (2019).
[21] M. Liu, L. Tan, S. Cao, Cavitation–Vortex–Turbulence Interaction and One-Dimensional Model Prediction of Pressure for Hydrofoil ALE15 by Large Eddy Simulation, Journal of Fluids Engineering 141(2) (2019).
[22] Y. Hao, L. Tan, Symmetrical and unsymmetrical tip clearances on cavitation performance and radial force of a mixed flow pump as turbine at pump mode, Renew. Energy, 127 (2018).
[23] Y. Liu, L. Tan, Tip clearance on pressure fluctuation intensity and vortex characteristic of a mixed flow pump as turbine at pump mode, Renew. Energy 129 (2018).
[24] M. Liu, L. Tan, S. Cao, Theoretical model of energy performance prediction and BEP determination for centrifugal pump as turbine, Energy 172(1) (2919).
[25] P. M. Singh, Z. Chen, Y. Hwang, M. Kang, Y. Choi, Performance characteristic investigation and stay vane effect on Ns100 inline francis turbine. Journal of the Korean Society of Marine Engineering 40(5) (2016) 397-402.
[26] Y. Nakamura, H. Komatsu, S. Shiratori, R. Shima, S. Saito, K. Miyagawa, Development of high-efficiency and low-cost shroudless turbine for small hydropower generation plant, ICOPE 2015 - International Conference on Power Engineering (2015).

[27] I. Samora, V. Hasmatuchi, C. Münch-Alligné, M.J. Franca, A.J. Schleiss, H.M. Ramos, Experimental characterization of a five blade tubular propeller turbine for pipe inline installation, Renewable Energy 95 (2016) 356–366.
[28] E. Vagnoni, L. Andolfatto, S. Richard, C. Münch-Alligné, F. Avellan, Hydraulic performance evaluation of a micro-turbine with counter rotating runners by experimental investigation and numerical simulation, Renewable Energy, 126 (2018) 943-953.
[29] D. Biner, V. Hasmatuchi, D. Violante, S. Richard, S. Chevailler, L. Andolfatto, F. Avellan, C. Münch-Alligné, Engineering & Performance of DuoTurbo: Microturbine with Counter-Rotating Runners, IOP Conference Series Earth and Environmental Science 49(10) (2016).R. Adhikari, D. Wood, The design of high efficiency crossflow hydro turbines: A review and extension, Energies 11(2) (2018).
[30] V. Sammartano, M. Sinagra, P. Filianoti, T. Tucciarelli, A Banki-Michell turbine for in-line hydropower systems, Journal of Hydraulic Research 55(5) (2017) 686-694.
[31] M. Sinagra, V. Sammartano, G. Morreale, T. Tucciarelli, A new device for pressure control and energy recovery in water distribution networks, Water (Switzerland) 9 (5) (2017).
[32] V. Sammartano, G. Morreale, M. Sinagra, T. Tucciarelli, Numerical and experimental investigation of a cross-flow water turbine, Journal of Hydraulic Research, 54 (3) (2016) 321-331.
[33] V. Sammartano, C. Aricò, A. Carravetta, O. Fecarotta, T. Tucciarelli, Banki-Michell optimal design by computational fluid dynamics testing and hydrodynamic analysis. Energies 6(5) (2013) 2362–2385.
[34] O. K. Chopra, W. J. Shack, ASME, Review of the Margins for ASME Code Fatigue Design Curve - Effects of Surface Roughness and Material Variability. U.S. Nuclear Regulatory Commission Office of Nuclear Regulatory Research -Washington, DC. September 2003.
[35] V. Sammartano, C. Aricò, M. Sinagra, T. Tucciarelli, Cross-flow turbine design for energy production and discharge regulation, Journal of Hydraulic Engineering 141 (3) (2015).
[36] A. Carravetta, G. Del Giudice, O. Fecarotta, H.M. Ramos, Energy Production in Water Distribution Networks: A PAT Design Strategy, Water Resources Management 26 (2012) 3947–3959.
[37] J. Delgado, J.P. Ferreira, D.I.C. Covas, F. Avellan, Variable speed operation of centrifugal pumps running as turbines. Experimental investigation, Renewable Energy 142 (2019) 437-450.
[38] J. Brady, J. Gallagher, L. Corcoran, P. Coughlan, A. McNabola, Effects of long-term flow variation on microhydropower energy production in pressure reducing valves in water distribution networks, Journal of Water Resources Planning and Management 143 (3) (2017).
[39] M. Sinagra, C. Aricò, T. Tucciarelli, P. Amato, M. Fiorino, Coupled Electric and Hydraulic Control of a PRS Turbine in a Real Transport Water Network, Water 11(6) (2019).

Highlights

- Experimental tests of a new compact in-line turbine named PRS, with good efficiency values, up to 76%
- PRS turbine suitable for control pressure or discharge inside a water transport or distribution network
- Validation of 3D CFD model for further improvement of the proposed turbine